View metadata, citation and similar papers at
brought to you by CORE
provided by Erasmus University Digital Repository

Piotr A. Wielopolski, PhD
Jochen Gaa, MD
Damian R. Wielopolski, M
Matthijs Oudkerk, MD, Ph

Index terms:
Bile ducts, MR, 76.121412, 76.121416
Pancreatic ducts, MR, 77.121412, 77.121416

Radiology 1999; 210:247–252

Abbreviations:
MRCP = MR cholangiopancreatography
RARE = rapid acquisition with relaxation enhancement
RF = radio-frequency
SE = spin-echo
SNR = signal-to-noise ratio
3D = three-dimensional

[1] From the Department of Radiology, Daniel den Hoed Kliniek, University Hospital Rotterdam, Groene Hilledijk 301, 3075EA Rotterdam, the Netherlands (P.A.W., M.O.); the Department of Radiology, University Hospital Mannheim, Germany (J.G.); and the Traumatology Department, Hospital Jesus Yerena de Lidice, Caracas, Venezuela (D.R.W.). Received October 30, 1997; revision requested January 6, 1998; final revision received June 4; accepted August 10. **Address reprint requests to** P.A.W.

© RSNA, 1999

Author contributions:
Guarantors of integrity of entire study, P.A.W., J.G., M.O.; study concepts and design, P.A.W.; definition of intellectual content, P.A.W.; literature research, P.A.W., D.R.W.; clinical studies, P.A.W., J.G.; experimental studies, P.A.W.; data acquisition and analysis, P.A.W., J.G.; statistical analysis, P.A.W., J.G.; manuscript preparation, P.A.W., D.R.W.; manuscript editing, P.A.W., J.G.; manuscript review, P.A.W., M.O.

Breath-hold MR Cholangiopancreatography with Three-dimensional, Segmented, Echo-planar Imaging and Volume Rendering[1]

End-expiration, 21-second breath-hold, three-dimensional magnetic resonance (MR) cholangiopancreatography (MRCP) was developed with segmented echo-planar imaging. In 15 healthy subjects and 14 randomly selected patients undergoing liver studies, three-dimensional MRCP images were obtained and volume rendered. In 15 (100%) healthy subjects and 13 (93%) patients, clear depiction of biliary, hepatic, and pancreatic ducts (with lumen diameter of at least 2 mm) was possible with good signal-to-noise ratio.

Fast magnetic resonance (MR) imaging techniques exploit the long T2 exhibited by biliary and hepatic fluids (>1.5 seconds) to produce high-quality, two- and three-dimensional (3D) MR cholangiopancreatographic (MRCP) images without the addition of contrast media. In initial attempts to visualize the entire biliary tree, steady-state free-precession imaging was used, with high contrast over several breath holds (1,2). However, steady-state free-precession sequences proved too sensitive to signal loss from magnetic susceptibility, fluid motion, and pulsation. More robustness is now possible with rapid acquisition with relaxation enhancement (RARE) (3) and fast spin-echo (SE) (4) sequences. With long effective echo times, only fluid-filled compartments are observed with nearly complete background suppression and minimal sensitivity to motion and signal loss due to magnetic susceptibility. Many techniques have been evaluated that differ in coverage, spatial resolution, signal-to-noise ratio (SNR), examination length, and patient cooperation. These techniques include breath-hold, two-dimensional, single-shot, single-projection, thick-section RARE (5); breath-hold, two-dimensional, multisection, half-Fourier RARE (HASTE; Siemens Medical Systems, Erlangen, Germany) (6); and fast SE (7,8) and respiratory-gated 3D fast SE (9,10). The RARE and half-Fourier RARE techniques have been widely explored and accepted as techniques of choice for diagnostic MRCP.

Nonetheless, the availability of a 3D fast SE technique would enable operator-independent imaging, large-volume coverage, examinations with maximum patient comfort, and the possibility of data reformation and volume rendering. Unfortunately, imaging time can still be excessive and results hampered by blurring from remnant respiratory motion. By combining 3D fast SE and segmented echo-planar imaging (11), we attempted to increase SNR and resolution in shorter imaging time, equivalent to an increase in data density, to obtain breath-hold volume images of the entire hepatic, bile, and pancreatic duct systems with the advantages of 3D acquisitions. Therefore, we performed this study to illustrate the potential of this new acquisition technique.

Materials and Methods

Patient Population

The study population included 15 healthy volunteers (six men, nine women; age range, 21–34 years). In addition, 14

patients were recruited randomly from those referred for abdominal MR studies before surgical intervention (nine men, five women; age range, 23–67 years). Of these 14 patients, six had normal duct anatomy, five had chronic pancreatitis, and three had tumor-related obstruction of the biliary tree; the gallbladder had been previously removed in four. The institutional review boards approved the study, and informed consent was obtained from all participants. Subjects were not required to fast before the examination.

MRCP Sequence

Figure 1 is a diagram of the 3D MRCP sequence. As in fast SE, multiple refocusing 180° radio-frequency (RF) pulses are applied after the initial 90° RF excitation. Between the 180° RF pulses, a number of echoes are read by using an echo-planar imaging readout and mapped along the in-plane phase-encoding direction by means of an interleaved k-space trajectory (12,13). For each 180° RF pulse, a single section-select phase-encoding step (partition) is encoded. The number of 180° RF pulses applied is equal to the number of partitions selected. A chemical-selective, fat-suppression pulse presides each 90° RF excitation (binomial excitation, 1331 [underlining indicates a 180° shift in the phase of the RF pulse]) to suppress fat and increase background suppression. The effective echo time and acquisition time are set according to the number of echoes, the number of partitions selected, and the echo spacing between the 180° RF pulses (Appendix).

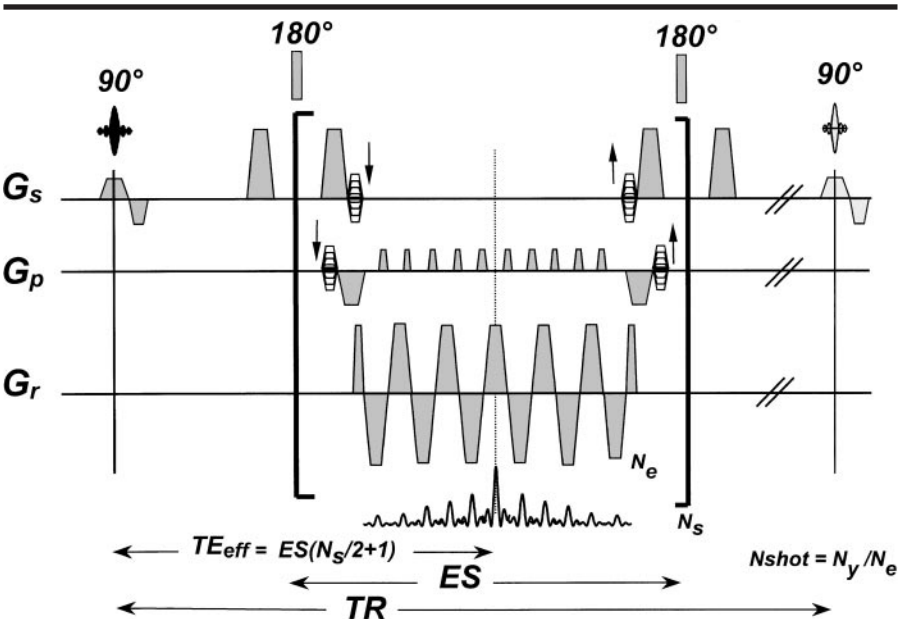

Figure 1. The 3D MRCP acquisition with a 3D RARE segmented echo-planar sequence. An echo-planar readout is placed between the string of 180° RF pulses to shorten the imaging time by a factor of the number of echoes in each echo-planar train (N_e). The echoes are phase encoded along the in-plane phase-encoding direction by using a blipped interleaved trajectory. The number of 180° pulses applied is equal to the number of sections encoded (N_s). The section-select phase-encoding table is performed sequentially to enable a long effective echo time (TE_{eff}). A chemical-shift-selective, fat-saturation pulse (not shown) is applied before each 90° RF excitation. *ES* = echo spacing (interval between 180° refocusing pulses), G_p = in-plane phase-encoding gradient, G_r = readout gradient, G_s = section-select gradient, $Nshot = N_y/N_e$, N_y = number of in-plane phase-encoding lines, *TR* = effective repetition time.

Imaging Protocol

The study was performed on a 1.5-T imager (Magnetom Vision; Siemens Medical Systems) with use of the body coil for RF excitation and a four-channel quadrature body phased-array coil. The 3D MRCP sequence was implemented with a maximum gradient strength of 25 mT/m and a gradient rise time of 300 μsec (83 T/m/sec).

Subjects were positioned supine and imaged with the body phased-array coil over the liver. Nonselective shimming was performed to increase magnetic field homogeneity. A conventional liver examination was performed before 3D MRCP for the patients. The acquisition parameters for 3D MRCP included the following: matrix size, 66 × 256; typical slab thickness, 80 mm; 64 sections (minimum section thickness, 1 mm); rectangular field of view ratio, 0.5; maximum in-plane resolution, 1.8 × 1.0 mm. The repetition time was set to 3.2 seconds, resulting in a 21-second breath hold, and imaging was performed at end expiration. With an 11-echo, echo-planar readout (echo spacing, 1.280 msec; bandwidth, 940 Hz per pixel), the interval between 180° refocusing pulses was 19.8 msec and the effective echo time was 653 msec. A 7.680-msec 90° RF excitation was used to select each slab, and 1-msec nonselective refocusing 180° RF pulses were applied to reduce RF power deposition. Presaturation bands were placed above and below the imaging volume to suppress the signal from incoming blood and undesired signals arising from imperfect 180° refocusing RF pulses outside the imaging volume. One or several volumes were concatenated (25% overlap) depending on liver size or desired section thickness.

Breath-hold quality was assessed immediately on a coronal and a transverse maximum intensity projection image after reconstruction. On the raw transverse sections or on a transverse maximum intensity projection image, the presence of bile fluid ghosting along the in-plane phase-encoding direction over the liver was indicative of inadequate breath holding and was used as the main criterion for repeat acquisition of the same image.

Image Analysis

The presence of artifacts (susceptibility, geometric distortion and ghosting), available SNRs, and the degree of background suppression were assessed by a physicist (P.A.W.) on the images obtained in all subjects. Mean signal intensities were obtained for fluids from the raw transverse sections at the closest and farthest locations possible from the receiver coils. Circular regions of interest were placed over the main hepatic duct or the proximal portion of the gallbladder to the cystic duct (or to the closest fluid-containing structure if any was present) and over the cerebrospinal fluid in the spinal canal. The minimum diameter of regions of interest was 4 mm. The properties of cerebrospinal fluid were assumed to match those of bile fluids. To compute the degree of background suppression, the liver signal intensity was measured by using a circular region of interest (15 mm diameter) placed in a region close to the center of the right hepatic lobe that did

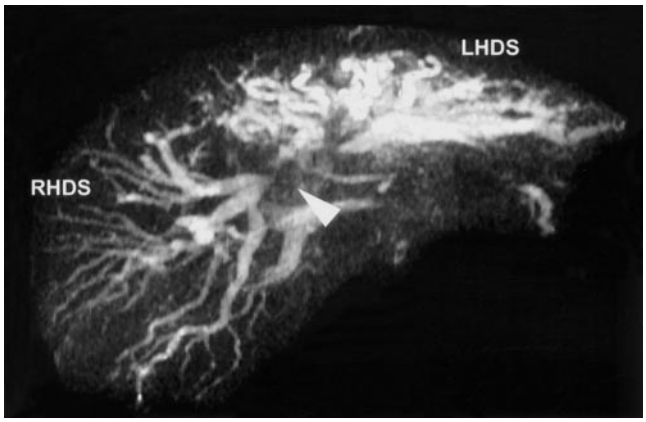

a.

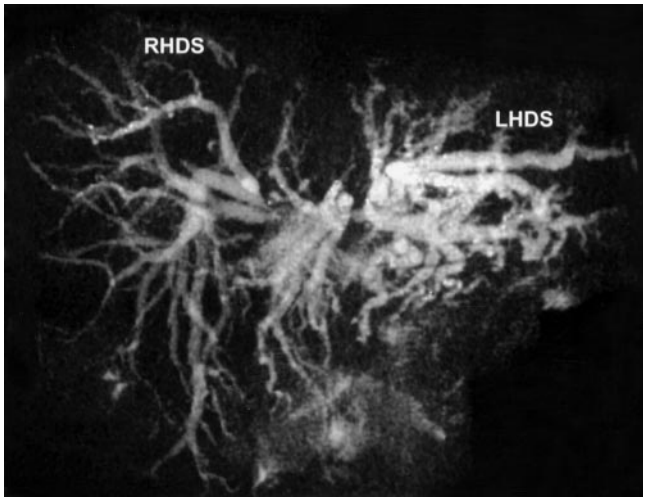

b.

Figure 2. **(a)** Transverse and **(b)** coronal oblique volume-rendered images obtained in a patient with pancreatic cancer and multiple large (1–5-cm diameter) liver metastases. The arrowhead in **a** indicates a large metastasis that obstructs the common bile duct and causes marked dilation of the right and left hepatic duct systems (*RHDS* and *LHDS*, respectively). Three 64-mm-thick slabs were concatenated to cover the entire liver (~180 mm long) in three 21-second breath holds. Sixty-four sections were encoded per volume (repetition time msec/effective echo time msec = 3,200/653; echo spacing, 19.8 msec; in-plane resolution, 2.5 × 1.25 mm).

not contain signal from fluids or noticeable artifacts. The mean intensity of the background noise was recorded to calculate SNR.

Images in several projections and section thicknesses were obtained from the 3D MRCP data by using maximum intensity projection and volume rendering. Branch visualization was retrospectively assessed and judged qualitatively in concert by two readers, a physicist (P.A.W.) and a radiologist (J.G.). The data were considered of good quality if cystic, pancreatic, or hepatic ducts with lumen diameters of at least 2 mm were clearly visualized. Pathologic confirmation was not performed. Volumes could be manipulated interactively on the imaging console by means of the standard processing platform for maximum intensity projection (while the patient remained in the imager). Volume rendering was applied to improve data visualization and reading. A software package (VoxelView; VitalImages, Minneapolis, Minn) was used on a commercially available workstation (Indigo2; Silicon Graphics, Mountain View, Calif). Bright structures surrounding the liver and pancreas—such as fluids in the gastrointestinal tract, kidneys, and ureters—were segmented before volume rendering. Data transparency was set to obtain a pseudoradiographic projection (similar to the resultant image in a RARE acquisition) to help distinguish overlapping or hidden features in the ducts. Thirty volume-rendered images were produced and reviewed in a cine loop (spanning 180° with 6° viewing angle increments). Structure segmentation by means of vessel tracking (placing a seed [starting point] in the unwanted structure and connecting all contiguous voxels within a range of signal intensity values) was used occasionally for fast tissue removal to reduce overlap between structures on images acquired in different viewing directions.

Results

Findings at breath-hold 3D MRCP demonstrated the expected fluid enhancement similar to that reported with other two-dimensional and 3D fast SE (RARE) MRCP implementations. In cases of obstruction caused by stones, stenosis, or tumor infiltration, intrahepatic ducts were best appreciated when they were depicted as dilated and could be observed throughout the entire liver.

In subjects with normal duct anatomy, one 80-mm-thick section was sufficient to cover the region of interest. For 13 of the 14 patients with pathologic findings in the routine liver examination, two overlapped 80-mm-thick sections were used to cover the entire liver. In the remaining patient, use of three volumes was necessary (18-cm craniocaudal excursion). As a result of qualitative assessment for the presence of ghosting or blurring on the raw transverse sections and on the transverse maximum intensity projection image, data collection was repeated in one volume in two patients and in two volumes in two other patients. The breath-hold time was accepted well by all but one patient, in whom good image quality was not possible after three breath-hold attempts. On the basis of a lack of abrupt mismatch between the volumes loaded into the maximum intensity projection or volume-rendering platforms, breath-hold position was consistent in 12 (80%) of the 15 volunteers and 10 (71%) of the 14 patients.

For all 15 (100%) volunteers, 3D MRCP images had good image quality. In all cases, the gallbladder, common bile duct, and second-order hepatic duct branches were observed. The pancreatic duct was observed in only 13 (87%) volunteers, however, as a result of its smaller size and higher sensitivity to blurring and increased background signal intensity from induced pulsation and peristalsis.

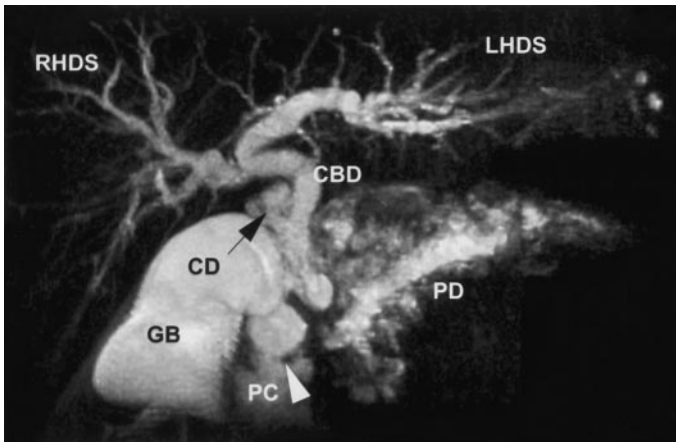

a.

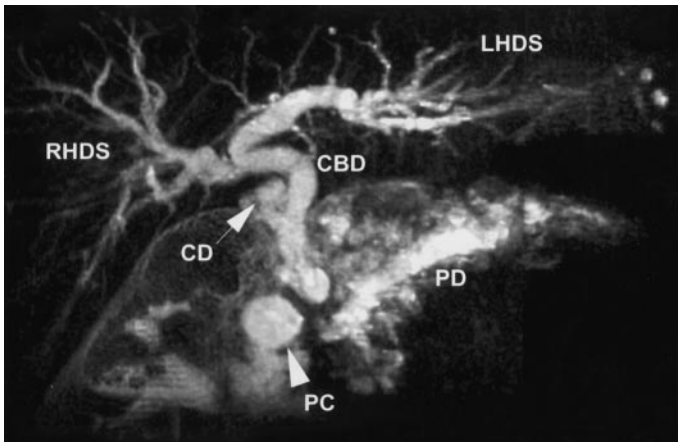

b.

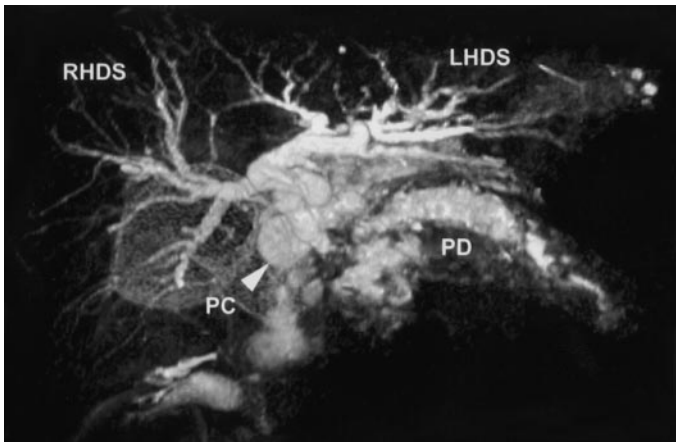

c.

Figure 3. Volume-rendered images obtained in a patient with chronic pancreatitis. **(a)** Coronal oblique image depicts a pseudocyst (*PC*, arrowhead), which is depicted more clearly on **(b)** a craniocaudal image acquired after gallbladder (*GB*) segmentation by means of vessel tracking. The arrow indicates the cystic duct (*CD*). **(c)** Transverse image depicts the right hepatic duct system (*RHDS*) more clearly after the gallbladder was segmented. Two 80-mm-thick slabs were concatenated to cover the entire liver in two 21-second breath holds. Sixty-four sections were encoded (3,200/653; echo spacing, 19.8 msec; in-plane resolution, 2.3 × 1.17 mm). *CBD* = common bile duct, *LHDS* = left hepatic duct system, *PD* = pancreatic duct.

Among the 13 patients included in the evaluation, the pancreatic duct was seen in 11 (85%). The pancreatic duct was severely obscured by ghosting from bowel fluids in one patient and was too small to be visualized in its full length in the other. Six (46%) of the patients had chronic pancreatitis, and the cystic duct was detected in 10 (77%). A remnant cystic duct was present in three of the four patients who had undergone cholecystectomy. The common bile duct was patent in 12 (92%) patients. Good image quality (ie, clear visualization of all ducts with lumen diameter of at least 2 mm) was achieved for all 13 (100%) patients. Intrahepatic branches were seen in all 13 (100%) patients, and abnormal duct dilatation was seen in eight (62%).

The SNR in regions of interest for fluids away from the coil (in the liver center) and on the cerebrospinal fluid were 6.8 ± 3.5 (mean ± SD) and 9.9 ± 3.9, respectively. The signal intensity of liver was similar to that of the background noise, yielding a mean SNR of 1.00 ± 0.05. In three cases, fluids close to the diaphragm were partially suppressed as a result of the application of the chemical-shift-selective, fat-suppression pulse.

Several examples demonstrate the quality of the volume-rendered images possible with the proposed 3D MRCP sequence. Figure 2 contains volume-rendered images obtained in a patient with pancreatic cancer and large liver metastases. Figure 3 illustrates volume-rendered images obtained in a patient with chronic pancreatitis. In Figure 3c, vessel tracking was used to provide fast segmentation of the gallbladder and improved depiction of the right hepatic duct system on a craniocaudal image. Figure 4 contains volume-rendered images obtained in a patient with chronic pancreatitis that clearly depict marked dilatation of the pancreatic duct and duct irregularities in the pancreatic tail. On average, data transfer, segmentation, and acquisition of 30 volume-rendered images could be performed in approximately 20 minutes.

Discussion

Although conventional endoscopic retrograde cholangiopancreatography, or ERCP, offers superior spatial resolution, RARE or half-Fourier RARE MRCP are becoming strong contenders, rivaling the conventional examination, with 512-matrix acquisitions (0.5 × 0.5-mm in-plane resolution) in any projection, noninvasively and with minimal patient collaboration. The breath-hold 3D MRCP sequence cannot yet provide this resolution, but if features fast volumetric imaging and an operator-independent setup with clear diagnostic results. Volumetric imaging makes it possible to reconstruct any plane with multiplanar reformatting and to produce volume-rendered images that illustrate the confluence of bile ducts, obstructions caused by stones, and stenotic regions. This is a major advantage as compared with RARE MRCP as it bypasses the need for acquisition of many projections with different section thicknesses to target a possibly problematic region (especially in cases with dilated ducts and overprojection). Similarly, as with some two-dimensional techniques, such as half-Fourier RARE, breath-hold 3D MRCP does not require extended imaging time, making the technique an adjunct to any two-dimensional examination that could help to target a particular

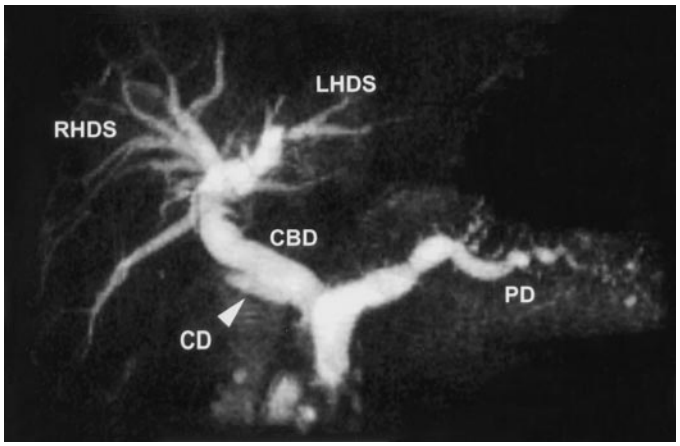

a.

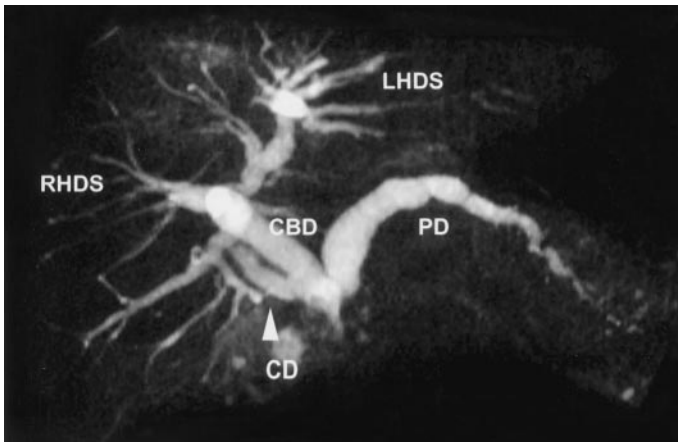

b.

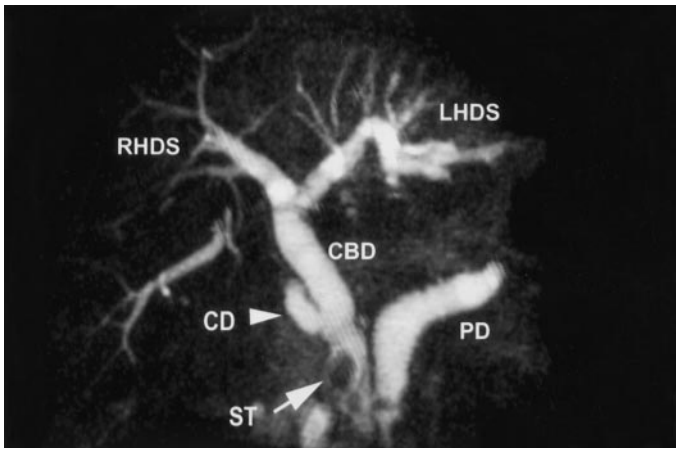

c.

Figure 4. Volume-rendered images obtained in a patient with chronic pancreatitis who had undergone cholecystectomy. **(a)** Coronal oblique and **(b)** transverse images depict a dilated pancreatic duct (*PD*) with marked irregularities and an enlarged cystic duct (*CD*, arrowhead). **(c)** Targeted thin-section image demonstrates a large stone (*ST*, arrow) in the common bile duct (*CBD*, arrow). Two 80-mm-thick slabs were concatenated to cover the entire liver in two 21-second breath holds. Sixty-four sections were encoded (3,200/653; echo spacing, 19.8 msec; in-plane resolution, 2.3 × 1.17 mm). *LHDS* = left hepatic duct system, *RHDS* = right hepatic duct system.

region. However, processing time must be longer to produce the best 3D display. It is important to consider use of other MR imaging techniques to demonstrate anatomic relationships if 3D MRCP is used alone for fluid visualization.

Image Artifacts

Breath-hold imaging implies patient cooperation. The short breath-hold time for two-dimensional MRCP makes the technique extremely robust and provides high in-plane resolution even in uncooperative patients. However, if image quality were not satisfactory, 3D MRCP could be repeated at will, a possibility that is not available with 3D fast SE implementations. In thin patients or those with substantial pathologic tissue, breath holds could be shortened to 15 seconds with use of a magnetization recovery period of 1 second, and adequate SNR would be achieved.

Similarly, as in multishot fast SE imaging, inadequate breath holds produce discrete ghosting along the in-plane phase-encoding direction (anteroposterior on transverse images). This was seen sporadically in cases of a large gallbladder with its anterior portion lying close to the receiving coils. Ghosting and blurring could be noted with fluids affected by peristalsis and heart pulsation. Agents such as glucagon could be used to further reduce artifacts by suppressing peristalsis (14). Ghosting from pulsation of cerebrospinal fluid was occasionally present and could be effectively suppressed by means of a presaturation band over the spinal canal.

Slow-moving blood could be noted over the background noise in several cases. This results from the presence of remnant signal during the collection of the center of k space and edge enhancement artifacts (with a T2 of 250 msec for blood, approximately 8% of signal would appear at an effective echo time of 650 msec with complete magnetization recovery and stationary blood). Blood did not interfere with image quality as the signal from fluid was several fold higher.

Geometric Distortion and Signal Loss from Magnetic Susceptibility

The 3D MRCP sequence benefits from the immunity of RARE and fast SE to slow flow dephasing. However, use of echo-planar imaging readouts makes the images more sensitive to geometric distortions and signal loss from susceptibility effects between air-tissue interfaces and metallic stents. It is advantageous that the center of k space is collected as a SE signal, and the signal loss present for the 11-echo implementation at the edges of k space is equivalent to an echo time of 6.4 msec in a conventional gradient-echo measurement. Additionally, use of small voxels and high readout bandwidths with large frequency-encoding gradients reduces signal loss and geometric distortions even further.

Fat Suppression

Chemical-shift-selective fat suppression is currently applied in fast SE–based MRCP techniques, with short and long effective echo times, to increase the contrast between fluids and surrounding fat or to suppress edge artifacts and ghosting that may arise from fat near the receiver coils at the beginning of the echo train (5–10). The application of chemical-shift-selective, fat-suppression techniques is not strictly necessary with the long effective echo time used in 3D MRCP and

would avoid possible fluid saturation in cases of poor homogeneity of the main magnetic field. In any case, the combination of chemical-shift fat suppression and echo-planar imaging requires the use of local shimming for optimal results.

Increased Acquisition Speed and SNR

Incorporation of the oscillatory echo-planar imaging readout produces an extra speedup factor proportional to the number of echoes encoded, making breath holding possible. Despite high readout bandwidths, the long T2 of fluid and the nature of the 3D acquisition compensate for any loss in SNR. A 3D acquisition introduces an improvement in SNR proportional to the square root of the number of sections acquired. A longer recovery interval between readouts (longer repetition time) produces better fluid enhancement, as more longitudinal magnetization is available for each readout train. This is possible only at the expense of an extended breath hold and risks for potential artifacts from inconsistent breath holding. Currently with repetition time of 3.2 seconds, the time for magnetization recovery for fluids is approximately 1.9 seconds, a signal recovery of approximately 38% between readouts with a T1 of 4 seconds. Additional SNR can be gained with use of faster gradient rise times. Shortening of the encoding time can extend the magnetization recovery period for the same breath-hold time or it could be used to shorten the acquisition.

Heat Power Deposition

Fast SE images can have large specific absorption ratios and produce large heat power deposition. The specific absorption ratio is reduced with use of fewer refocusing 180° RF pulses with increased spacing. Because this 3D MRCP technique makes use of an echo-planar readout, the number of refocusing 180° RF pulses is effectively reduced while the long RF spacing can be maintained, which results in lower specific absorption ratios (15). The use of nonselective refocusing 180° RF pulses reduces specific absorption ratios even further.

Future Improvements

The 3D MRCP data display sufficient SNR to allow half-Fourier reconstruction and improved resolution along either the in-plane or section-select phase-encoding directions or shortened imaging time (approximately 10 seconds for the current implementation). Currently, multiple volumes are used to cover the entire liver. The use of half-Fourier reconstruction could offset this by allowing acquisition of a single volume with extended coverage or by allowing isotropic imaging with a 1-mm^3 minimum voxel size (currently, $1.8 \times 1.0 \times 1.0$ mm). Multislab capability with use of selective refocusing 180° RF pulses can also be envisioned to increase volume coverage and to increase sampling efficiency (continuous data collection), with longer recovery time for fluids, for an eventual increase in SNR.

In conclusion, breath-hold 3D MRCP with segmented echo-planar imaging can deliver fast imaging of the bile duct system. Display after volume rendering offers the ability to view the data from multiple directions, which may eventually prove clinically useful in such areas as planning of interventional procedures or understanding of complex relationships between pathologic and normal duct anatomy.

Appendix

For any fast SE sequence, the effective echo time (TE_{eff}) is defined by the time interval between the initial 90° RF excitation and the SE formed at the center of k space. For the current 3D implementation with segmented echo-planar imaging along the in-plane phase-encoding direction and sequential section-select phase encoding, the center of k space is defined by the center section-select phase-encoding value. Defining the echo spacing (ES) as the time interval between the refocusing 180° RF pulses, $TE_{eff} = ES(N_s/2 + 1)$, where N_s is the number of section-select phase-encoding steps (partitions) employed and the term in parentheses is the center partition. The acquisition time, T_{acq}, is approximately $TR(N_y/N_e) + (ES \times N_s)$, where N_y is the number of in-plane phase-encoding lines, N_e is the number of echoes encoded between refocusing pulses, and TR is the repetition time between shots. The number of shots is related to the ratio N_y/N_e, but an additional excitation is included in T_{acq} to obtain the projection data (navigator echo) that corrects all hardware-related misalignments that may occur between the alternating echoes in the echo-planar imaging train.

Acknowledgments: The authors thank former colleagues at the Beth Israel Deaconess Medical Center, Boston, Mass, specifically, William Buff, MD, and Melvin Clouse, MD, for their interest in breath-hold volumetric MRCP, and Bart Schraa, MRT, for his help in patient imaging.

References

1. Morimoto K, Shimoi M, Shirakawa T, et al. Biliary obstruction: evaluation with three-dimensional MR cholangiography. Radiology 1992; 183:578–580.
2. Ishizaki Y, Wakayama T, Okada Y, Kobayashi T. Magnetic resonance cholangiography for evaluation of obstructive jaundice. Am J Gastroenterol 1993; 88:2072–2077.
3. Hennig J, Nauerth A, Friedburg H. RARE imaging: a fast imaging method for clinical MR. Magn Reson Med 1986; 3:823–833.
4. Mulkern RV, Wong ST, Winalski C, et al. Contrast manipulation and artifact assessment of 2D and 3D RARE sequences. Magn Reson Imaging 1990; 8:557–566.
5. Laubenberger J, Büchert M, Schneider B, et al. Breathhold projection magnetic resonance-cholangio-pancreaticography (MRCP): a new method for the examination of the bile and pancreatic ducts. Magn Reson Med 1995; 33:18–23.
6. Fulcher AS, Turner MA, Capps GW, et al. Half-Fourier RARE MR cholangiopancreatography: experience in 300 subjects. Radiology 1998; 207:21–32.
7. Takehara Y, Ichijo K, Tooyama N, et al. Breath-hold MR cholangiopancreatography with a long-echo-train, fast spin-echo sequence and a surface coil in chronic pancreatitis. Radiology 1994; 192:73–78.
8. Guibaud L, Bret PM, Reinhold C, et al. Diagnosis of choledocholithiasis: value of MR cholangiography. AJR 1994; 163:847–850.
9. Barish MA, Yucel EK, Soto JA, et al. MR cholangiopancreatography: efficacy of three-dimensional turbo spin-echo technique. AJR 1995; 165:295–300.
10. Soto JA, Barish MA, Yucel EK, et al. MR cholangiopancreatography with a three-dimensional fast spin-echo technique. Radiology 1995; 196:459–464.
11. Wielopolski PA, Zuo C, Clouse M, Buff B. Breathhold 3D cholangiography using RARE and segmented echo planar imaging readouts (abstr). In: Proceedings of the Third Meeting of the International Society for Magnetic Resonance in Medicine. Berkeley, Calif: International Society for Magnetic Resonance in Medicine, 1995; 1448.
12. McKinnon GC. Ultrafast interleaved gradient-echo-planar imaging on a standard scanner. Magn Reson Med 1993; 30:609–616.
13. Butts K, Riederer SJ, Ehman RL, Thompson RM, Jack CR. Interleaved echo planar imaging on a standard MRI scanner. Magn Reson Med 1994; 31:67–72.
14. Marti-Bonmati L, Graells M, Roncheras-Oms CL. Reduction of peristaltic artifacts on magnetic resonance imaging of the abdomen: a comparative evaluation of three drugs. Abdom Imaging 1996; 21: 309–313.
15. Feinberg DA, Oshio K. GRASE (gradient- and spin-echo) MR imaging: a new fast clinical imaging technique. Radiology 1991; 181:597–602.